Journal of Applied Polymer Science

Mechanical, Electrical, and Dielectric Properties of Polyvinylidene Fluoride/Short Carbon Fiber Composites with Low-Electrical Percolation Threshold

Ranvijai Ram, Mostafizur Rahaman,* Dipak Khastgir*

Rubber Technology Centre, Indian Institute of Technology Kharagpur, Kharagpur, 721302, West Bengal, India

*Present address: Chemical Engineering Department, King Fahd University of Petroleum and Minerals, Dhahran, 31261, Eastern Province, Kingdom of Saudi Arabia

Correspondence to: M. Rahaman (E-mail: mrahaman1997@gmail.com) or D. Khastgir (E-mail: khasdi@rtc.iitkgp.ernet.in)

ABSTRACT: In this investigation, polyvinylidene fluoride (PVDF)/short carbon fiber (SCF) composites have been prepared by solution casting technique to enhance electrical and dielectric properties with very low-electrical percolation threshold (0.5 phr SCF). The effect of SCF content on mechanical, thermal and morphological properties of the composites have also been investigated. The mechanical properties of the composites are found to reduce compared to neat PVDF due to poor polymer–filler interaction which can be concluded from FESEM micrographs showing poor bonding between PVDF and SCF. The PVDF/SCF composites exhibit either positive temperature coefficient effect of resistivity or negative temperature coefficient effect of resistivity depending on the loading of SCF in the polymer matrix. The change in conductivity during heating–cooling cycle for these composites shows electrical hysteresis along with electrical set. The melting point of the composites marginally increases with the increase in fiber loading in PVDF matrix as evidenced from DSC thermograms. X-ray diffraction analysis reveals the crystallinity of PVDF decreases with the increase in SCF loading in matrix polymer. © 2013 Wiley Periodicals, Inc. J. Appl. Polym. Sci. **2014**, *131*, 39866.

KEYWORDS: dielectric properties; differential scanning calorimetry (DSC); mechanical properties; X-ray; conducting polymers

Received 2 May 2013; accepted 17 August 2013
DOI: 10.1002/app.39866

INTRODUCTION

The mechanical, electrical, and dielectric properties of any filler–polymer composite can be controlled by varying filler to polymer proportion, state of filler distribution and dispersion in the matrix polymer, and filler geometry.[1–8] To achieve properties like mechanical reinforcement, electrical sensing, electromagnetic interference shielding effectiveness (EMI SE), good electric and dielectric properties, thermal properties in the polymer composite, it is necessary to mix and disperse the filler uniformly in the polymer matrix, which provides wetting of filler particles by polymer chains leading to a good bonding in between filler and polymer.[9–11] It is well documented that electrical, dielectric, mechanical or any other physical property of the polymer composites depend on the nature of polymer and filler individually.[12–20] There are several other factors like filler dispersion in polymer matrix,[21–23] physicochemical bonding in between polymer and filler,[24,25] polymer–polymer compatibility in case polymer blend is used as matrix,[26–29] electronic charactrestis of polymer and filler for example presence of lone pair or pi bond or both in conjugation in polymer,[30] duration of mixing time,[31–34] method of mixing,[35] aspect ratio of filler, temperature of mixing. All these factors affect the physical properties of polymer–filler composites. The electrical conductivity of conductive polymer composites also depends on temperature.[36] The electrical conductivity in insulating polymer is achieved by incorporating conductive fillers where electrical conductivity drastically increases up to a crtical concentration of filler known as percolation thresold.[37,38]

It is observed that EMI SE and toughness increase with increasing SCF concentration whereas rheological properties either in extrution or injection moulding process decreases.[39] The mixing of SCF in polyvinylidene fluoride (PVDF) matrix produces a low adhesion due to lack of reactive groups and innert nature of PVDF, that results in poor mechanical properties of PVDF/SCF composite.[40,41]

The objective of this research work is to develop PVDF/SCF (aspect ratio = 735) composites having high electrical conductivity at low percolation threshold. To fulfil this objective, PVDF and SCF composites have been prepared by solution mixing method.

The effect of SCF loading on mechanical properties, dielctric properties, both ambient and temperature dependent electrical resistivity, and crystallinity, have been investigated and an effort

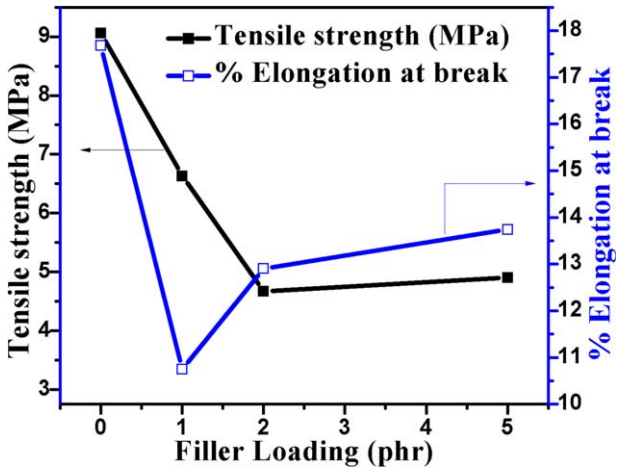

Figure 1. TS and elongation at break of PVDF/SCF composites. [Color figure can be viewed in the online issue, which is available at wileyonlinelibrary.com.]

is made to correlate composite structure with different properties through SEM morphology, X-ray diffraction (XRD) and differential scanning calorimetry (DSC) analyeses.

EXPERIMENTAL

Materials

Conductive carbon fiber (RK 30/12) was obtained from RK Carbon Fibers, UK. Short carbon fiber (SCF), having average length of 5 mm was prepared by chopping continuous carbon fiber. It has diameter = 6.8 μm, density = 1.78 g/cm^3, electrical resistivity = 1.5 $\times$ 10^{-3} Ω cm, and aspect ratio = 735. The PVDF [average molecular weight (M_w), 534,000] was supplied by Aldrich, USA, under the trade name 182702 and has a density of 1.77 g/cm^3. *N*,*N*-dimethyl formamide (DMF) was used as a solvent for PVDF which was obtained from Merk Specialities, Worli, Mumbai.

Sample Preparation

Different PVDF/SCF composite films were prepared by solution casting method. The clear and saturated solution of PVDF in *N*,*N*-DMF was initially prepared. Different proportion of chopped SCF particles with average length of 5 mm was mixed and sonicated for 30 min with requisite amount of saturated solution of PVDF. The mixture was again mechanically mixing for extra half an hour. Composite films were prepared through casting of different mixtures of PVDF and SCF on Petri dish followed by drying in vacuum oven at 40°C for 48 h.

Characterization

Tensile properties of PVDF/SCF composites have been measured by Hounsfield universal mechanical testing machine (UTM), H10KS with loading cell at the testing speed 5 mm/min.

Crystalline melting temperature of different composites was measured using DSC (Q100 T.A. Instruments, USA) under N_2 atmosphere, over a temperature range −70 to 210°C at a heating rate of 10°C per minute. XRD was carried out by using Philips PW 1710 diffractometer, angle (2θ) ranges from 10° to 80° to study the effect of SCF length on composite's crystallinity.

DC electrical resistivity measurement at ambient temperature (25 ± 2°C) was performed using Agilent 4339B high resistance meter [coupled with Agilent 16008B resistivity cell (for samples having electrical resistance $\geq 10^6$ Ω)] and Agilent 34401A 6½ digital multimeter [couples with a homemade electrode (for samples having electrical resistance $\leq 99 \times 10^6$ Ω)]. The dielectric constant, dielectric loss and AC resistivity in the frequency range from 10 to 10^6 Hz were measured using QuadTech 7600 precision LCR meter attached with a homemade electrode.

The effect of temperature (30–150°C) on DC resistivity of PVDF/SCF composites were measured using the instrument Agilent 34401A 6½ digital multimeter. The entire electrode with sample was placed in an electrically heated oven (SC Dey Company). The temperature was maintained through PDI controller attached with the oven. The effects of heating and heating–cooling cycle on DC resistivity were done at the heating–cooling rate 1°C/min. But the effect of heating and heating–cooling rate (speed) on DC resistivity and electrical hysteresis has been carried out at two different rates namely 1 and 5°C/min.

Leica, DMLM-P-11888500 (Germany) optical microscopy and SUPRA 40 field emission scanning electron microscope (FE-SEM) were used for understanding morphology and distribution of SCF in PVDF matrix.

RESULTS AND DISCUSSION

Mechanical Properties

The tensile strength (TS) of SCF-filled PVDF composites are presented in Figure 1. It can be seen from the figure that as the concentration of SCF increases from 0 to 2 phr, there is a continuous decrease in TS whereas for 2–5 phr SCF loading variation there is only marginal increase in TS. This reveals that SCF acts as nonreinforcing filler for PVDF matrix unlike carbon black. Carbon black generally acts as reinforcing filler for elastomeric matrices. But in present case, SCF acts as nonreinforcing filler. This is because carbon black has some active groups like >CO, —COOH, —CHO, —OH, etc., which helps in the formation of some kind of physicochemical bonds with polymer matrix. However, SCF surface does not contain any such groups as, during manufacturing of carbon fiber it was subjected to very high temperature leading to destruction of such groups on SCF surface. Further carbon black surface has some roughness as well as black particles generally exist in aggregated and agglomerated form which leads to formation of some kind of mechanical interlocking between polymer chains and carbon black particles. SCF surface on the other hand is much more smooth compared to carbon black as a result there is a much less tendency to form some mechanical locking between SCF particles and polymer chains.[3] Consequently, physicomechanical bonds between polymer chains and SCF particles are rather weak compared to that in carbon black-polymer bond. The existence of poor SCF-polymer interaction has also been reported elsewhere.[42]

Jianghong et al. have studied the reinforcement effect of carbon fiber (CF, with and without surface treatment) on the mechanical properties of PVDF matrix prepared through melt mixing

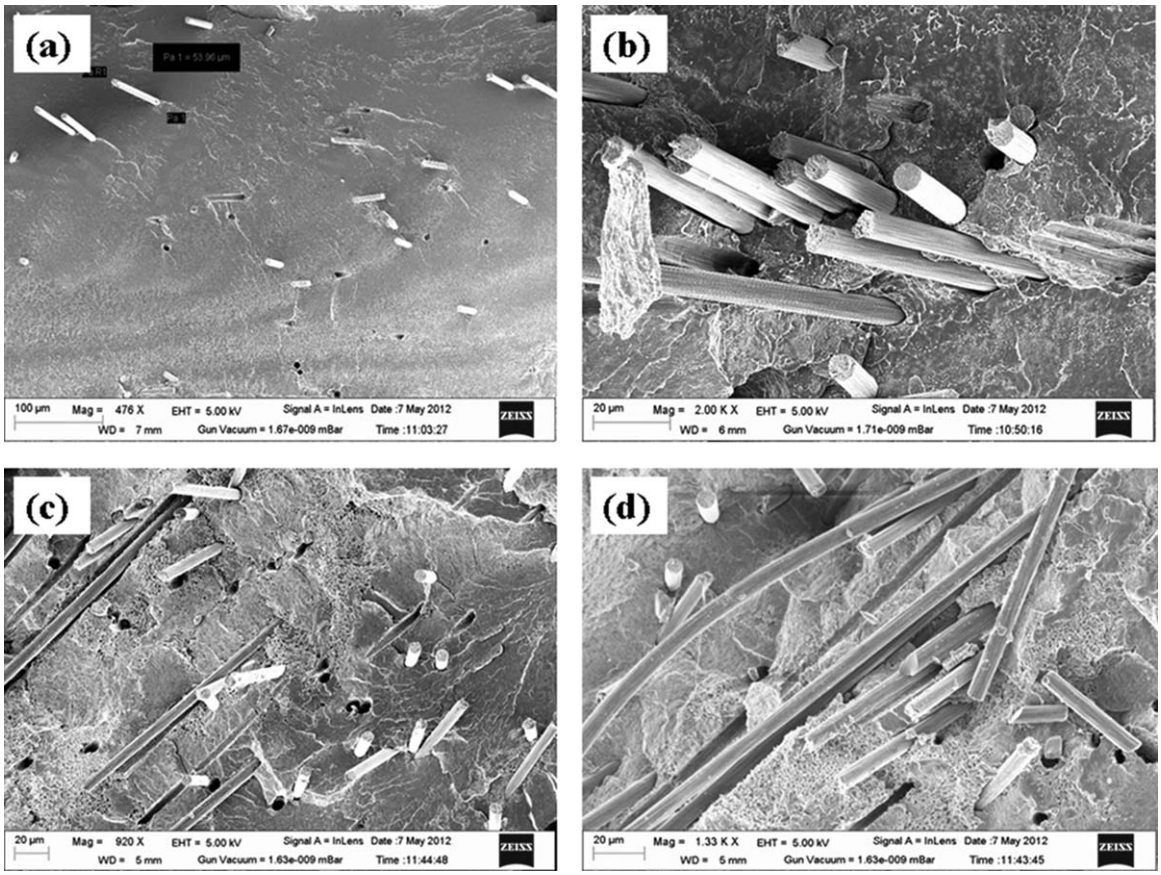

Figure 2. FESEM images of cryo-fractured PVDF/SCF composite (a–d).

technique.[43] They have reported that, with the increase in CF loadings up to 28 wt %, the TS of the composites was increased by about 180% compared to neat polymer. The discrepancy in between earlier report and present findings is mainly due to due to the difference in methods of composite preparation and the of carbon fiber surface treatment. Unlike present case of composite preparation through solution mixing using SCF without any surface treatment, melt mixing process was adopted by Jianghong et al. using surface treated SCF. However, this reduction in mechanical properties is well compensated by comparatively much better improvement in electrical conductivity at much lower filler loading in the present case.

The variation of elongation at break against SCF loading (Figure 1) shows somewhat similar trend as that observed for TS. Because of SCF addition in PVDF matrix the elongation at break is found to decrease up to loading of 1 phr there after a marginal change is observed for increase in filler loading from 2 to 5 phr.

The FESEM images of PVDF/SCF composite shown in Figure 2(a–d). It is observed that fibers have been pulled out from matrix polymer creating holes and channels on the polymer surface. It is also noteworthy that de-bonded fiber surfaces are smooth and do not exhibit presence of any polymer on them. This provides an ample evidence of weak bonding between PVDF and SCF in the composite system.[3]

DC Resistivity

The DC resistivity of SCF-loaded PVDF composites has been presented in Figure 3. It can be seen from the figure that initially the resistivity is reduced drastically with the addition of very small amount of SCF in PVDF matrix. The resistivity of the composites decreases from 10^{14} (for neat polymer) to 10^{6} Ω cm at the loading of only 0.5 phr of SCF which is further reduced to 10^{4} Ω cm when loading is increased upto 1 phr. However, for further increase in SCF loading even up to 5 phr, there is only marginal decrease in resistivity. Here, the electrical percolation (the critical concentration of filler) which causes the transition of the composite from insulating to semiconducting/conducting is taking place at and around 0.5 phr of SCF. The retention of initial high aspect ratio (L/D) of SCF during composite preparation through solution mixing followed by solvent casting helps in the formation of continuous conducting network of SCF in PVDF matrix even at very low loading, 0.5 phr.

These PVDF/SCF composites are found to be superior to many similar polymer composites prepared using the same SCF, as mentioned earlier literature. Sau et al. reported percolation threshold value ranging from 14 to 30 phr for different for SCF (SCF, aspect ratio = 13–30) filled nitrile rubber (NBR), ethylene propylene diene rubber (EPDM) and their blend composites.[44] The percolation threshold value of 8–10 vol % (16.3–20.8 phr) were observed for polypropylene (PP)/SCF composites (SCF,

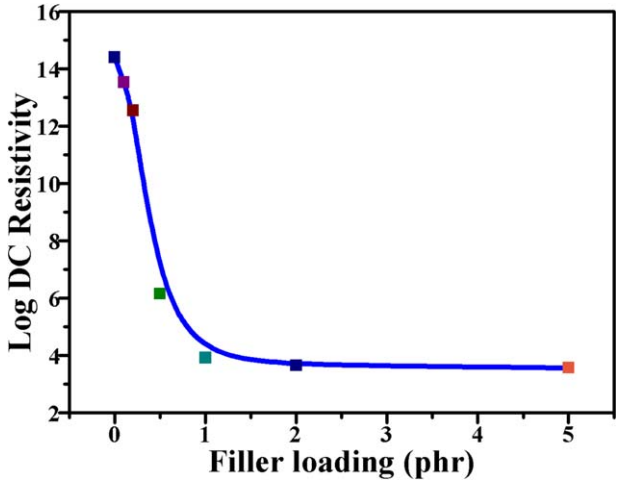

Figure 3. DC resistivity of PVDF/SCF composites against filler loading. [Color figure can be viewed in the online issue, which is available at wileyonlinelibrary.com.]

aspect ratio = 24).[45] The achieving of high conductivity level with very low percolation threshold for the present SCF-PVDF is noteworthy. Li et al. reported electrical percolation for PVDF/EG composites system as 8 phr (6 vol %) significantly higher than present composite system.[46] Better electrical conductivity for the present PVDF/SCF composites is mainly due to initial high aspect ratio of SCF (735) which almost retained in final composites which facilitate the formation of continuous conductive networks inside the matrix polymer at very low percolation threshold.

Optical microscopic images of composites reveals percolation the formation of continuous conductive networks as shown in Figure 4(a–f), mostly the SCF particles are randomly distributed in PVDF matrix. At a concentration (<0.5 phr), SCF particles remain separated from each other [Figure 4(b,c)] in PVDF matrix but with progressive increase in SCF concentration the average interpartcle gap decreases and a tendency of continuous network formation is aparent. Initially, the network is not continuous but slowly the formed network spreads and becomes continous at and around critical concentration [Figure 4(d)] and the system changes abruptly from insulating to conducting one. However, with further addition of SCF in the system more and more closed packed networks are formed [Figure 4(e,f)].

The effect of temperature on DC resistivity and relative resistivity of PVDF/SCF composites has been shown in Figures 5 and 6, respectively. The term relative resistivity is defined as ρ_t/ρ_0, where ρ_t is the resistivity at any measurement temperature and ρ_0 is the resistivity at the starting temperature (30°C). It is observed from Figure 5 that the resistivity of 1 and 2 phr SCF loaded composites increases with the increase in temperature (the positive temperature coefficient, PTC effect) whereas, the 5 phr loaded composite exhibits different behavior where the resistivity is found to decrease with the increase in temperature

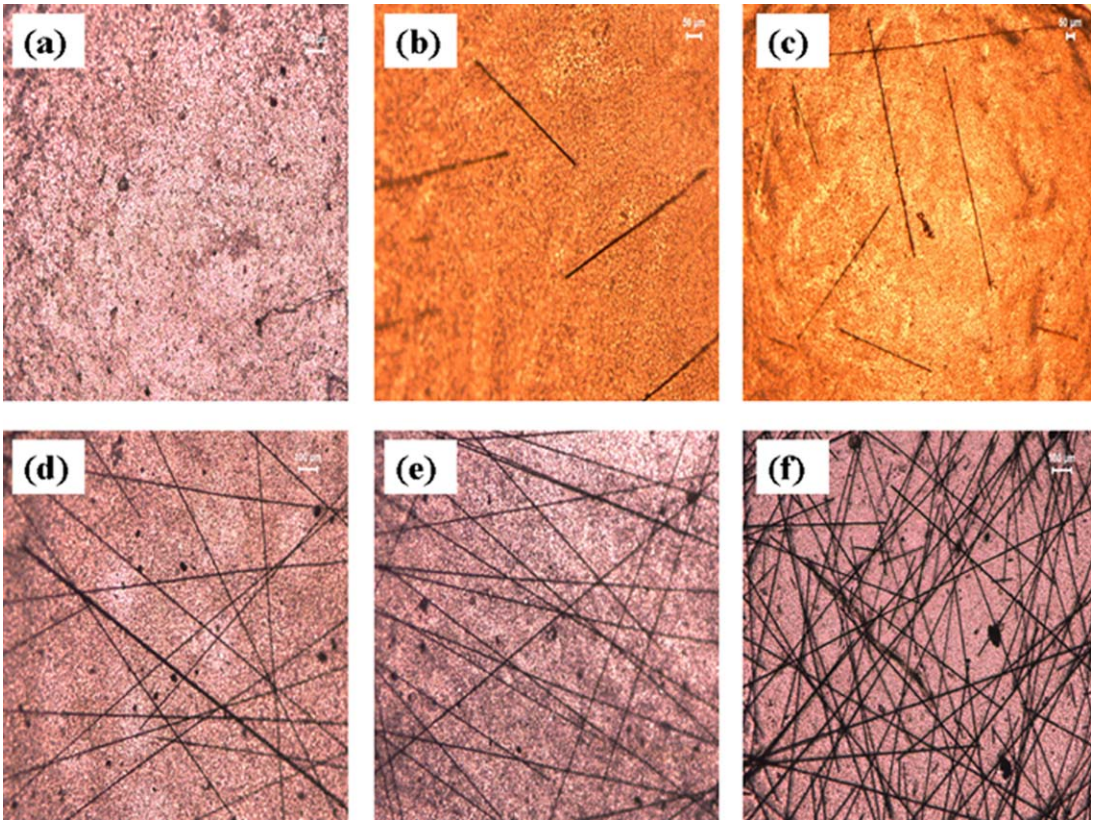

Figure 4. Distribution of SCFs in PVDF matrix (a) 0.0 phr SCF, (b) 0.1 phr SCF, (c) 0.2 phr SCF, (d) 0.5 phr SCF, (e) 1.0 phr SCF, and (f) 2.0 phr SCF. [Color figure can be viewed in the online issue, which is available at wileyonlinelibrary.com.]

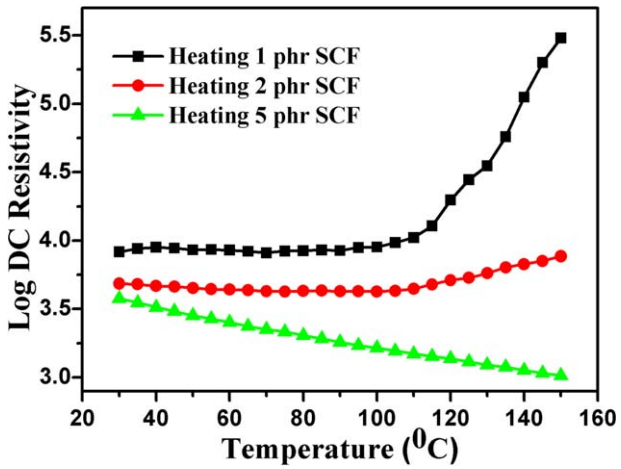

Figure 5. DC resistivity against temperature of PVDF/SCF composites. [Color figure can be viewed in the online issue, which is available at wileyonlinelibrary.com.]

(negative temperature coefficient, NTC effect). The appearance of PTC or NTC effects respectively depends on the net increase or net decrease of conductive networks of filler present in the composite which in turn depends on the nature of matrix polymer, type of conductive filler and filler concentration. PTC effect is generally due to higher thermal expansion of polymer matrix compared to filler leading to net destruction whereas NTC effect is due to the increased effect of electric field radiation between adjacent conductive filler particles in the matrix which bridges the interparticle gap and facilitates network formation. In fact with the increase in temperature, the electrons present in the composite system especially in the conductive fillers radiate from one conductive site to another in the matrix when the conductive sites are close enough and around 10 Å, resulting in better electron flow and reduction in electrical resistivity.

In the present composite system the carbon fiber has negative coefficient of thermal expansion (-1.45×10^{-6})[47,48] whereas the matrix PVDF has positive thermal expansion coefficient $(+7.1 \times 10^{-5})$.[49] Because of this difference in thermal expansion between filler and matrix, average interparticle gap increases and resistivity increases that is what is observed a for composites with 1 and 2 phr SCF loaded composites. Whereas comparatively highly loaded (5 phr) composite where there are more number of conductive networks already present and average interparticle gap is also much less compared to previous ones, the effect of differential thermal expansion is marginal. But the decrease in resistivity is mainly due to increased effect of electric field radiation which predominate the increase in resistivity by thermal expansion. The relative increase in resistivity for 2 and 5 phr loaded composite is lower compared to 1 phr loaded composite. The change in relative resistivity for 1 phr loaded composite is from 1 to 1.45, for 2 phr loaded composite is from 1 to 1.04, and for 5 phr loaded composite is from 1 to 0.84. Li et al. reported that the relative resistivity of the PVDF/EG composites increases with the increase in temperature up to the melting point of PVDF that is the PTC effect of resistivity is observed for the composite system.[46] The increment in relative resistivity is in the order of 10^1 to 10^3 depending on the loading of EG. For the present system the close packed networks of SCF in PVDF matrix exhibits much lower variation of relative resistivity against temperature compared to previous results.

The effects of heating–cooling and repeated heating–cooling cycle on DC resistivity have been shown in Figure 7 for 1 and 5 phr loaded composites. It is observed that the change in resistivity during heating does not follow the same root during cooling part of the heating cycle leading to some kind of hysteresis and the original value of resistivity at the starting temperature is not reached at the end of heating–cooling cycle leaving a difference in the resistivity value which may be termed as electrical set.[48] So it is clear from the figure that the composites show electrical hysteresis where there exist an electrical set. The electrical hysteresis is defined as the difference in area between resistivity versus temperature plots during heating and cooling

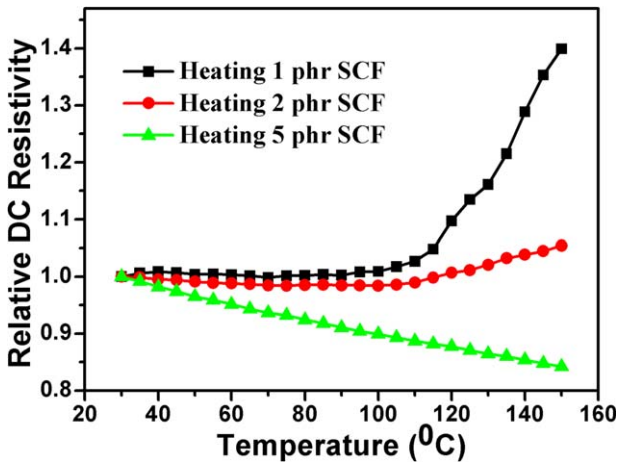

Figure 6. DC relative resistivity against temperature of PVDF/SCF composites. [Color figure can be viewed in the online issue, which is available at wileyonlinelibrary.com.]

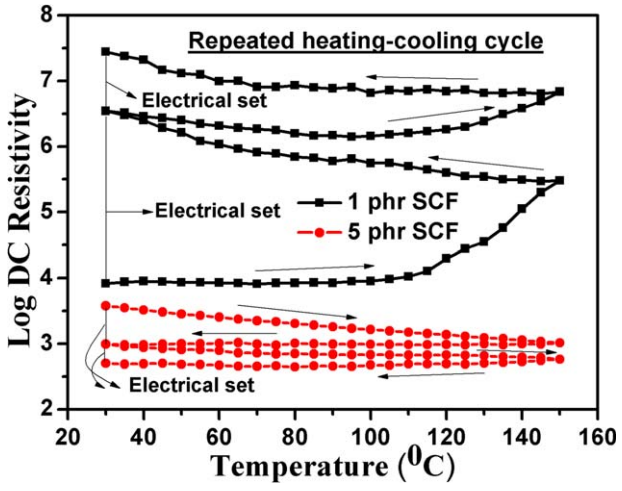

Figure 7. Repeated heating–cooling cycle for 1 and 5 phr loaded PVDF/SCF composites. [Color figure can be viewed in the online issue, which is available at wileyonlinelibrary.com.]

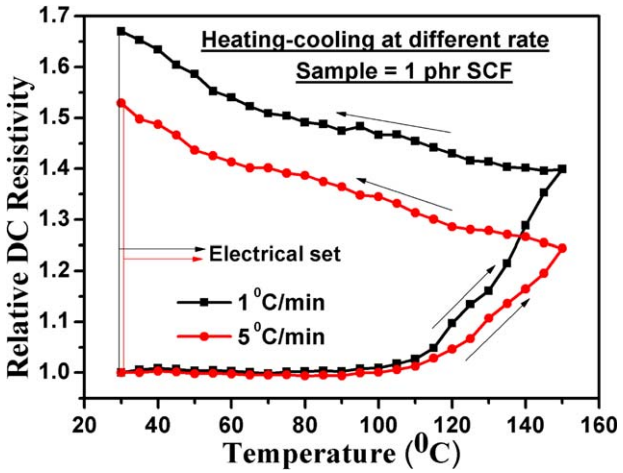

Figure 8. Effect of heating–cooling rate on DC resistivity for 1 phr loaded PVDF/SCF composite. [Color figure can be viewed in the online issue, which is available at wileyonlinelibrary.com.]

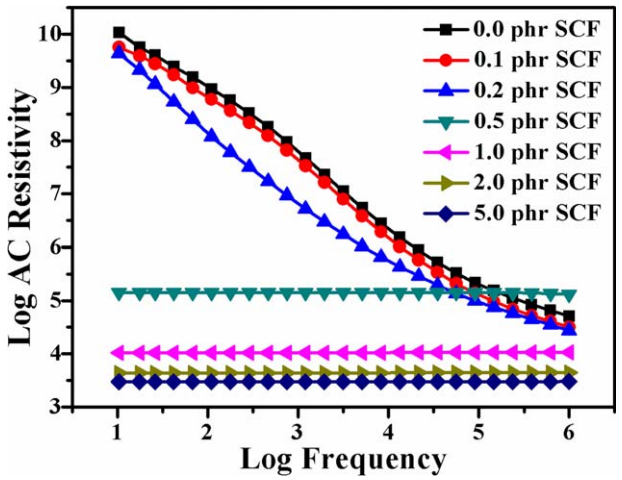

Figure 10. AC resistivity against frequency of PVDF/SCF composites. [Color figure can be viewed in the online issue, which is available at wileyonlinelibrary.com.]

cycle. The electrical set is the difference between initial resistivity at the starting temperature of the composite before heating–cooling cycle and final resistivity at the starting temperature after heating–cooling cycle. There is wide difference between the initial and final resistivity. But it is interesting to show that the final resistivity (after cooling) for 1 phr loaded composite is quite higher compared to initial resistivity; whereas, the final resistivity for 5 phr loaded composite is lower compared to its initial resistivity. The increase in final resistivity after heating–cooling cycle has also been observed by Sau et al, where the only difference was in the magnitude of electrical set.[44] It is also observed from the figure that the magnitude of electrical hysteresis and electrical set in the second heating–cooling cycle is less compared to first heating–cooling cycle. The effect of heating and cooling cycle on DC resistivity for 1 phr loaded composite have been measured at two different rates (1 and 5°C/min) and shown in Figure 8. It is seen from the figure that the DC resistivity is dependent on heating–cooling rate. The increase in heating–cooling rate decreases the electrical hysteresis and electrical set.

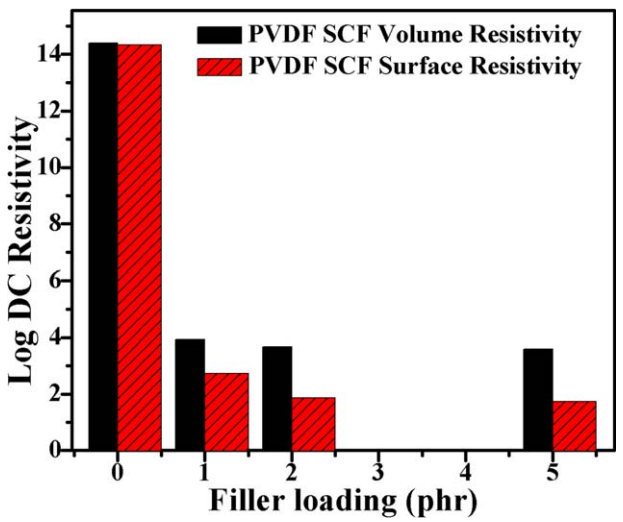

Figure 9. Comparison of volume and surface resistivity of PVDF/SCF composites. [Color figure can be viewed in the online issue, which is available at wileyonlinelibrary.com.]

A comparison between volume and surface resistivity of PVDF/SCF composites against filler loading is presented in Figure 9. It is observed that the magnitude of surface resistivity at any particular SCF loading is always lower than the corresponding volume resistivity. It may be due to the fact that the fibers tend to distribute more towards surface compared to the bulk of the PVDF matrix.

AC Resistivity

AC resistivity of different PVDF/SCF composites against logarithm of applied frequency is presented in Figure 10. It is found that when concentration of SCF is more or equal to the percolation thresold, the AC resistivity is frequency independent. It is clear from the figure that frequency dependent AC resistivity is observed for composites with 0–0.2 phr SCF loading but when SCF loading is increased to $\geq$0.5 phr (percolation thresold and above), the AC resistivity becomes almost frequency independent that is AC resistivity becomes equal to DC resistivity.

AC Resistivity of different PVDF/SCF composite against their filler loading are presented in Figure 11. The effect of filler loading on AC resistivity is found to be similar to that of DC resistivity. The only difference is in their magnitude. The difference in AC resistivity at lower filler loading is due to the hopping/tunneling of electrons from one conductive site to another site. Generally hopping/tunneling phenomena increases with the increase in frequency.[14] This is why at lower filler loading, the AC resistivity measured at higher frequency exhibits lower value.

The AC conductivity for EVA/SCF composites has been reported by Sohi et al.[50] They have shown that the electrical percolation has reached around 15 phr of fiber loading, whereas, for this study, it is only 0.5 phr. Furthermore, in terms of AC resistivity, the present composite loaded with 1 phr SCF is found to be more effective compared to 20 phr loaded EVA/

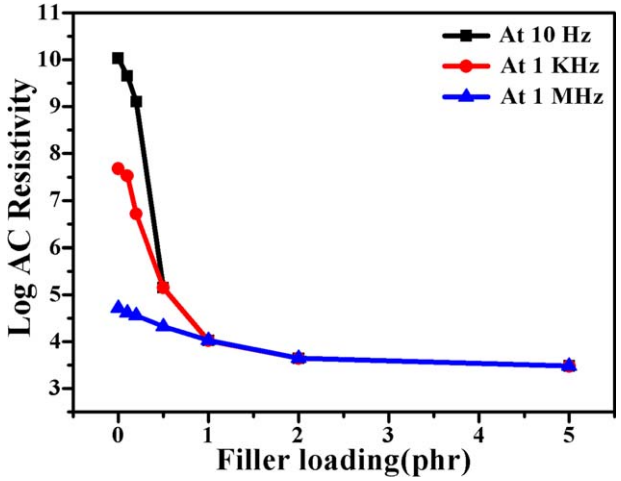

Figure 11. AC resistivity against filler loading of PVDF/SCF composites. [Color figure can be viewed in the online issue, which is available at wileyonlinelibrary.com.]

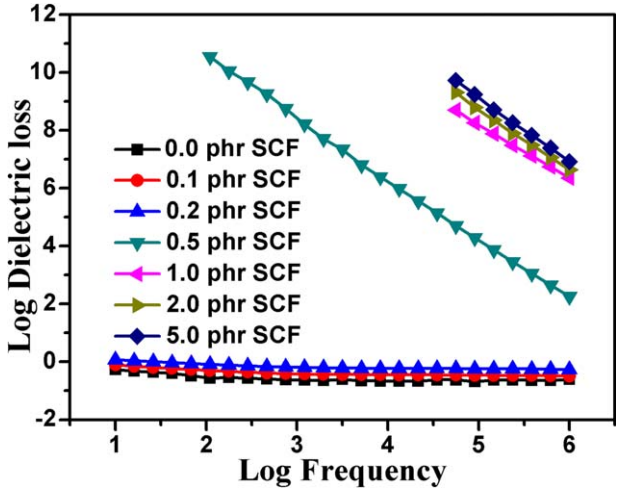

Figure 13. Dielectric loss against frequency of PVDF/SCF composites. [Color figure can be viewed in the online issue, which is available at wileyonlinelibrary.com.]

SCF composite. The percolation threshold of AC electrical conductivity for PVDF/EG composite system is around 8 phr of EG loading, which is higher compared to this study.[46] The electrical AC conductivity result of 0.5 phr loaded present PVDF/SCF composite is better compared to 8 phr loaded PVDF/EG composite.

Dielectric Constant and Loss

Dielectric constant and loss of different composites against log frequency is presented in Figures 12 and 13, respectively. The change in dielectric constant against frequency is marginal upto 0.2 phr SCF that is before percolation. When SCF loading is increased to 0.5 phr, dielectric constant almost linearly increases with decrease in log frequency upto log equal to 2. If the frequency is further lowered, measurement value is erratic and unreliable. For the composites having fiber loading above percolation threshold (>0.5 phr), the dielectric constant is found to increase almost linearly with the decrease in frequency from 10^6 to 5×10^4 Hz. But when the frequency is further decreased, the system become highly conducting and the dielectric constant value goes beyound the measurement limit of the instrument used.

The variation of dielectric constant and dielectric loss with respect to filler loading at constant frequency 1 MHz has been presented in Figures 14 and 15, respectively. From both the figure it is seen that the dielectric constant and loss are increasing with respect to filler loading. Initially upto 0.2 phr SCF loading, the increment is very marginal followed by a drastic increment in dielectric constant and dielectric loss upto 1 phr. Futher addition of SCF gives marginal increment.

The SCF present in the PVDF matrix can be considerd as milli capacitor which generates interfacial polarization with the polymer matrix and among themselves.[12,16] The increase in SCF loading increases such numbers of capacitors.[16] This results in

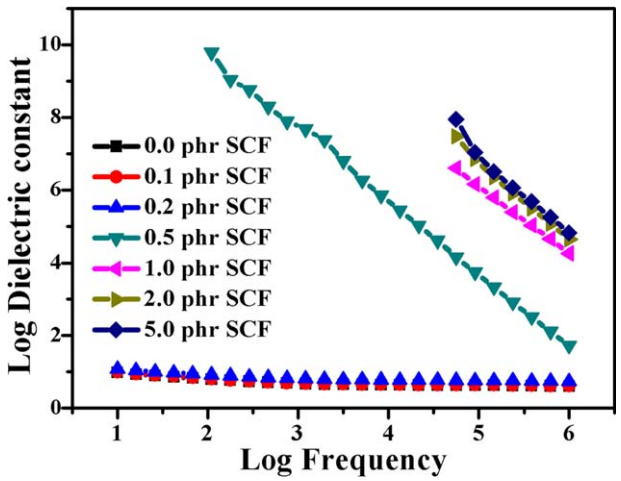

Figure 12. Dielectric constant against frequency of PVDF/SCF composites. [Color figure can be viewed in the online issue, which is available at wileyonlinelibrary.com.]

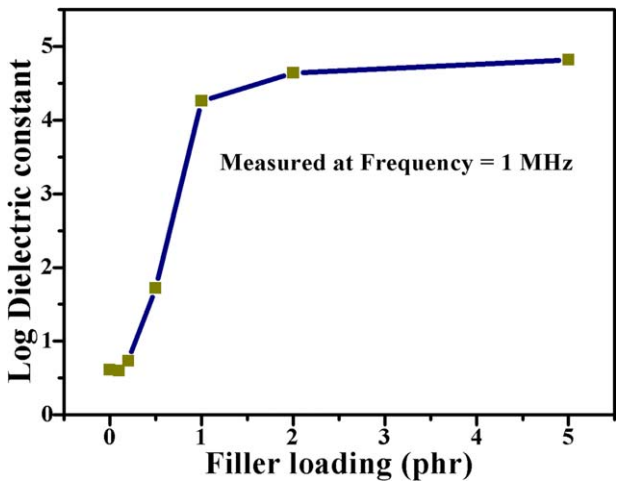

Figure 14. Dielectric constant against filler loading of PVDF/SCF composites. [Color figure can be viewed in the online issue, which is available at wileyonlinelibrary.com.]

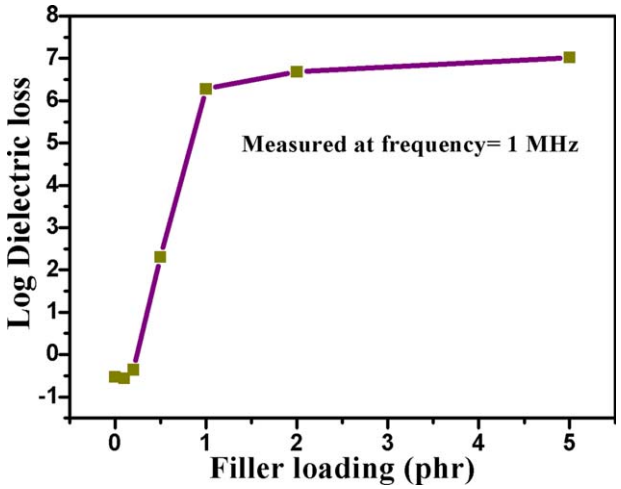

Figure 15. Dielectric loss against filler loading of PVDF/SCF composites. [Color figure can be viewed in the online issue, which is available at wileyonlinelibrary.com.]

higher magnitude of interfacial polarization especially at lower frequencies. This attributes to the increment of dielectric constant and loss with the increase in filler loading.

From Figures 14 and 15, it is observed that the magnitude of dielectric loss is higher compared to dielectric constant at the similar loading of SCF (specially for higher loaded composites). This is due to the higher value of dissipation factor (>1). Because dielectric loss is the product of dielectric constant and dissipation factor.

The dielectric property of similar SCF filled ethylene vinyl acetate (EVA) composites has been investigated by our previous group.[13] It is observed that the dielectric constant results of 1 phr loaded PVDF/SCF composite is higher compared to 15 phr loaded EVA/SCF composite. Similarly, the dielectric constant of 0.5 phr loaded PVDF/SCF composite is quite higher compared to 8 phr loaded PVDF/EG composite.[46] The dielectric constant for 0.5 phr loaded PVDF/SCF composite at log frequency 2 is in the order of 10^{10} whereas for 8 phr loaded PVDF/EG composite the dielctric constant is only in the order of 10^3. Dang et al. have investigated the dielectric constant of PVDF/upright carbon fiber composites.[51] They have reported that the dielectric constant at volume fraction 0.074 (7.99 phr) of carbon fiber (at log frequency 3) is around 80 (less than log 2) that is extremely lower compared to our 0.5 phr loaded PVDF/SCF composites. The credit for this high effective of PVDF/SCF composites goes to the high aspect ratio of SCF. Actually, a carbon fiber with higher aspect ratio may be considered as a series combination of several microcapacitor made of smaller carbon fiber. This is why the composite with higher aspect ratio of fiber exhibits higher dielectric property compared to the composite having lower aspect ratio of fiber.

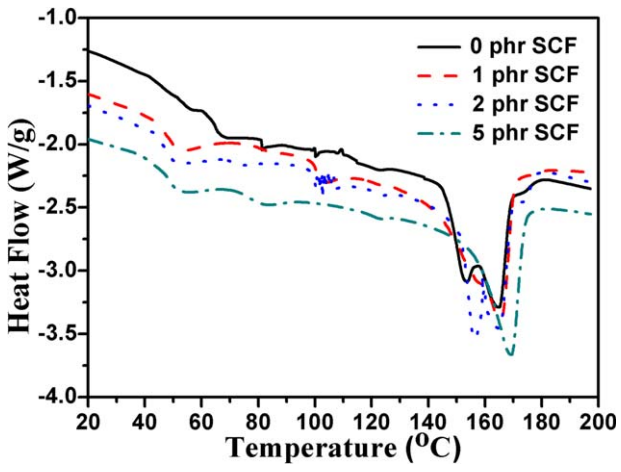

Figure 16. DSC thermogram of PVDF/SCF composites. [Color figure can be viewed in the online issue, which is available at wileyonlinelibrary.com.]

Differential Scanning Calorimetry

DSC plot of different SCF-filled PVDF composites are presented in Figure 16. The DSC curves show the melting endotherms of crystalline neat PVDF and PVDF/SCF composites from where the corresponding crystalline melting temperatures (T_m) can be clearly detected. A distinct transition around 50–60°C is observed for the PVDF composites. This may be due to some structural changes in PVDF matrix. In fact PVDF can exist in one to five different crystalline form[42] depending on the chain configuration. As a result it shows different types of transitions depending on the type of crystalline form. A sharp endothermic peak is observed for all systems at around 150–175°C. This is due to crystalline melting of PVDF matrix. There is marginal shift of melting peak with SCF loading is observed.

It is seen from Figure 16 that the melting point of 1 and 5 phr loaded composites are 165 and 170°C, respectively. These melting points are somewhat higher compared to the highest measurement temperature of DC resistivity as shown in Figure 6. It has been mentioned in literature that for the semicrystalline polymer composites (filled with any carboneous filler), the major increase in electrical resistivity occurs around the melting point of the composites.[46,52] But for 1 and 5 phr loaded PVDF/SCF composites, the highest measurement temperature are 15 and 20°C lower than their melting point, respectively. Thus, this may be one of the reasons for the very low increase/decrease of relative resistivity with respect to temperature compared to other carbon filled composites.

X-ray Diffraction Analysis

PVDF has five polymorphic forms viz. α, β, γ, δ, and ε in which conformation of alpha (α) and delta (δ) is TGTG′, gamma (γ) and epsilon (ε) is TTTGTTTG′, and beta (β) is TTTT.[53] XRD patterns of pure PVDF and PVDF—SCF composites have been shown in Figure 17. The peak obtained at around 2θ = 18.7°, 20.0°, and 26.4° reflect α-crystal structure which can be indexed into α (020), α (110), and α (021) for pure PVDF.[54–57] The absence of 2θ peak at around 20.6° shows that there is no formation of β-crystal structure during drying of solution casted pure PVDF. However, PVDF-SCF composites exhibit β-crystal structure.

The crystallinity for neat PVDF and its composites have been calculated using the following relation [eq. (1)].

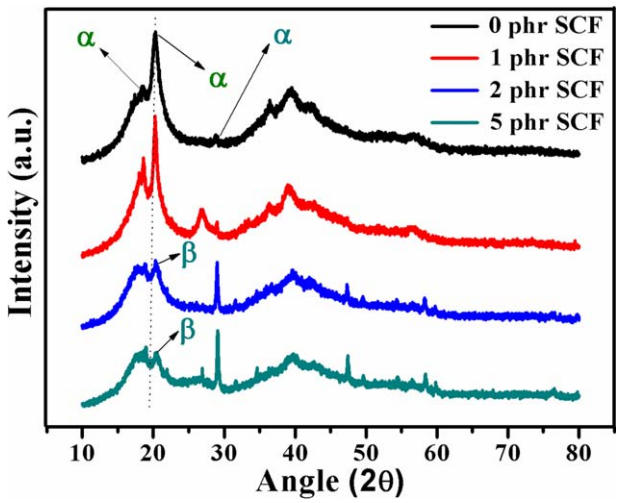

Figure 17. XRD analysis of PVDF/SCF composites. [Color figure can be viewed in the online issue, which is available at wileyonlinelibrary.com.]

$$\text{Crystallinity}(\%) = [\text{Cp}/(\text{Cp}+\text{Ap})] \times 100 \quad (1)$$

where Cp = Crystalline peak area and Ap = Amorphous peak area. It is found that the crystallinilty for neat PVDF, 1, 2, and 5 phr loaded PVDF-SCF composites is 51%, 45%, 44%, and 24% respectively. It has been mentioned earlier that there is no chemical interaction between PVDF and SCF because SCF has no functional group on its surface. Hence, the added SCF in the PVDF matrix only disturb the formation of parallel alignment of PVDF chain. This leads to decrease in crystallinity with increase of SCF loading in PVDF matrix.

SUMMARY AND CONCLUSIONS

The decrease in TS and elongation at break of the composite compared to neat PVDF is due to poor interaction between matrix PVDF and filler SCF. FESEM photo micrographs also corroborate the poor polymer–filler interaction. The electrical percolation has been found to be 0.5 phr of SCF loading which is significantly low compared to earlier reported results for similar composites. Dielectric constant and dielectic loss have been found to increase with increasing filler loading. For composites with filler loading less than percolation threshold, AC resistivity is frequency depedent whereas for composites having filler loading equal to or higher than percolation it is frequency independent which means AC and DC conductivity marges togather. PVDF/SCF composites exhibits either PTC or NTC effect of resistivity depending on filler loading. The DC resistivity shows electrical hysteresis along with electrical set. Both area under hysteresis loop and magnetude of electrical set decrease if heating–cooling cycle is repeated. Dielectric properties increase with the increase in SCF loading mainly due to the increase in interfacial polarisation and electronic conductivity especially at low-frequency region.

ACKNOWLEDGMENTS

R.R. thanks University Grant Commisssion (UGC) for providing fellowship to carry out this research work.

REFERENCES

1. Certeisen, S. R. *Eng. Plast.* **1996**, *9*, 26.
2. Kraus, G. *Rub. Chem. Technol.* **1965**, *38*, 1070.
3. Rahaman, M.; Chaki, T. K.; Khastgir, D. *Polym. Compos.* **2011**, *32*, 1790.
4. Weber, M.; Kamal, M. *Polym. Compos.* **1997**, *6*, 711.
5. Nayak, L.; Rahaman, M.; Khastgir, D.; Chaki, T. K. *Polym. Bull.* **2011**, *67*, 1029.
6. Chahal, R. S.; Pierre, L. E. St. *Macromolecules* **1968**, *1*, 152.
7. Rahaman, M.; Chaki, T. K.; Khastgir, D. *SPE, Plast. Res.* Online 2011, DOI: 10.1002/spepro.003964.
8. Dani, A.; Ogale, A. A. *Compos. Sci. Technol.* **1996**, *8*, 911.
9. Chahal, R. S.; Pierre, L. E. St. *Macromolecules* **1969**, *2*, 193.
10. Gale, R. L.; Beebe, R. A. *J. Phys. Chem.* **1964**, *68*, 555.
11. Chung, D. D. L. *Carbon* **2012**, *50*, 3342.
12. Krupa, I.; Chodak, I. *Eur. Polym. J.* **2001**, *37*, 2159.
13. Sohi, N. J. S.; Rahaman, M.; Khastgir, D. *Polym. Compos.* **2011**, *32*, 1148.
14. Lizhen, F.; Zhimin, D.; Ce-Wen, N.; Ming, L. *Electrochim. Acta* **2002**, *48*, 205.
15. Rahaman, M.; Chaki, T. K.; Khastgir, D. *Adv. Sci. Lett.* **2012**, *10*, 115
16. Yang, L.; Schruben, D. L. *Polym. Eng. Sci.* **1994**, *34*, 1109.
17. Kuljanin, J.; Vucković, M.; Cómor M. I.; Bibić, N; Djoković, V.; Nedeljković, J. M. *Eur. Polym. J.* **2002**, *38*, 1659.
18. Selvin, T. P.; Adedigba, A. A.; Mamdouh, A.; Muataz, A. A.; De, S. K.; Rahaman, M.; Chaki, T. K.; Khastgir, D.; Bandyopadhyay, S. *J. Mater. Sci.* **2012**, *47*, 3344.
19. Araujo, F. F. T.; Rosenberg, H. M. *J. Phys. D. Appl. Phys.* **1976**, *9*, 665.
20. Das, N. C.; Chaki, T. K.; Khastgir, D. *Carbon* **2002**, *40*, 807.
21. Premphet, K.; Horanont, P. *Polymer* **2000**, *41*, 9283.
22. Hornsby, P. R.; Premphet, K. *J. Appl. Polym. Sci.* **1998**, *70*, 587.
23. Rahaman, M.; Chaki, T. K.; Khastgir, D. *J. Mater. Sci.* **2011**, *46*, 3989.
24. Jing, X.; Zhao, W.; Lan, L. *J. Mater. Sci. Lett.* **2000**, *19*, 377.
25. Flandin, L.; Prasse, T.; Schueler, R.; Bauhoffer, W.; Schulfe, K.; Cavaillé, J. Y. *Phys. Rev. B* **1999**, *59*, 14349.
26. Shifrin, V. V.; Lipatov, Y. S.; Nesterov, A. Y. E. *Polym. Sci.* **1985**, *27*, 412.
27. Chiou, J. S.; Barlow, J. W.; Paul, D. R. *J. Polym. Sci. Part B: Polym. Phys.* **1987**, *25*, 1459.
28. Koo, K. K.; Inoue, T.; Miyasaka, K. *Polym. Eng. Sci.* **1985**, *25*, 741.
29. Kunori, T.; Geil, P. H. *J. Macromol. Sci. Part B: Phys.* **1980**, *18*, 93.
30. Hoeben, F. J. M.; Jonkheijm, P.; Meijer, E. W.; Schenning, A. P. H. *J. Chem. Rev.* **2005**, *105*, 1491−1546.
31. Borse, N. K.; Kamal, M. R. *Polym. Eng. Sci.* **2006**, *46*, 1094.
32. You-Ping, W.; Yong, M.; Yi-Qing, W.; Li-Qun, Z. *Macromol. Mater. Eng.* **2004**, *289*, 890.

33. Gatos, K. G.; Thomann, R.; Karger-Kocsis, J. *Polym. Int.* **2004**, *53*, 1191.
34. Dilhan, M. K.; Elvan, B.; Rahmi, Y.; Bahadir, K.; Shawn, W. *Polym. Eng. Sci.* **2002**, *42*, 1609.
35. Kan-Sen, C.; Kuo-Cheng, H.; Zong-Huai, S. *J. Appl. Polym. Sci.* **2005**, *97*, 128.
36. Rahaman, M.; Chaki, T. K.; Khastgir, D. *Adv. Mater. Res.* **2010**, *123*, 447.
37. Sandler, J. K. W.; Kirk, J. E.; Kinloch, I. A.; Shaffer, M. P.; Windle, A. H. *Polymer* **2003**, *44*, 5893.
38. Rahaman, M.; Chaki, T. K.; Khastgir, D. *Compos. Sci. Technol.* **2012**, *72*, 1575.
39. Guanghong, L.; Xiaotian, L.; Hancheng, J. *Compos. Sci. Technol.* **1996**, *56*, 193.
40. Marcos, Z.; Dan, D.; Henry, S. *Carbon* **1994**, *32*, 485.
41. Bismarck, A.; Tahhan, R.; Springer, J.; Schulz, A.; Klapötke, T. M.; Zell, H.; Michaeli, W. *J. Fluorine Chem.* **1997**, *84*, 127.
42. Park, S. J.; Papirer, E.; Donnet, J.B. *J. Chim. Phys. Phys.-Chim. Biol.* **1994**, *91*, 203.
43. Jianghong, W.; Defeng, W.; Xiang, L.; Ming, Z.; Weidong, Z. *Appl. Surf. Sci.* **2012**, *258*, 9570.
44. Sau, K. P.; Chaki, T. K.; Khastgir, D. *Polymer* **1998**, *39*, 6461.
45. Kalaitzidou, K.; Fukushima, H.; Drzal, L. T. *Materials* **2010**, *3*, 1089.
46. Li, Y. C.; Li, R. K. Y.; Tjong, S. C. *J. Nanomater.* **2010**, *34*, 10.
47. Sau, K. P.; Chaki, T. K.; Khastgir, D. *Polymer* **1998**, *39*, 6461.
48. Rahaman, M.; Chaki, T. K.; Khastgir, D. *J. Mater. Sci.*, **2013**, *48*, 7466.
49. Available at: http://www.plastic-products.com/pvdfspec.htm, accessed on February 20, 2013.
50. Sohi, N. J. S.; Bhadra, S.; Khastgir, D. *Carbon* **2011**, *49*, 1349.
51. Dang, Z. M.; Wu, J. P.; Xu, H. P.; Yao, S. H.; Jiang, M. J.; Bai, J. *Appl. Phys. Lett.* **2007**, *91*, 072912.
52. Kang, P. H.; Nho, Y. C. *J. Ind. Eng. Chem.* **2001**, *7*, 199.
53. Lovinger, A. J. *Science* **1983**, *220*, 1115.
54. Yu, S.; Zheng, W.; Yu, W.; Zhang, Y.; Jiang, Q.; Zhao, Z. *Macromolecules* **2009**, *42*, 8870.
55. Huang, X. Y.; Jiang, P. K.; Kim, C.; Liu, F.; Yin, Y. *Eur. Polym. J.* **2009**, *45*, 377.
56. Patro, T. U.; Mhalgi, M. V.; Khakhar, D. V.; Misra, A. *Polymer* **2008**, *49*, 3486.
57. Lanceros-M'endez, S.; Mano, J. F.; Costa, A. M.; Schmidt, V. H. *J. Macromol. Sci. Phys.* **2001**, *40*, 517.